Volume 3, Number 3, 2026 Pages 1-25

Bioscience Insights

ISSN: 3080-3489 (Print)
ISSN: 3080-3497 (Online)

BiosciInsights.com

CHITOSAN-TREATED SOLID LIPID NANOPARTICLES LOADED WITH ESSENTIAL OILS: PHYSICOCHEMICAL CHARACTERIZATION AND PRELIMINARY IN VITRO ANTIOXIDANT SCREENING

Amina Sehar[*1], Hira Mubeen[2], Madiha Riaz[3]

[*1,2]*Department of Biotechnology, Faculty of Science and Technology, University of Central Punjab, Lahore, Pakistan*

[3]*Institute of Molecular Biology and Biotechnology University of Lahore*

[*1]aminaseharleo26@gmail.com, [2]hira.mubeen@ucp.edu.pk, [3]madiha.riaz@imbb.uol.edu.pk

https://doi.org/10.5281/zenodo.24126041

Article Information

Article History

Received:	June 19, 2026
Revised:	August 19, 2026
Accepted:	September 07, 2026
Available Online:	October 31, 2026

Keywords:
Solid lipid nanoparticles; essential oils; chitosan; essential oil nanoencapsulation; dynamic light scattering; DPPH

Copyright @Author
Corresponding Author: *
Amina Sehar

Abstract

Diseases transmitted by mosquitoes continue to be a public health issue, leading to increased interest in plant-derived substitutes for artificial repellents. Essential oils show potential, yet their volatility restricts the duration of protection, and lipid nanoparticles could assist in transporting them. We formulated solid lipid nanoparticles (SLNs) containing a blend of three oils: Melissa officinalis, Lavandula angustifolia, and Eucalyptus globulus oils, and assessed uncoated SLNs against chitosan-treated SLNs (CSLNs). Chitosan treatment decreased the total hydrodynamic diameter from 410.3 to 245.2 nm, tightened the size distribution (PDI 21.6% to 16.3%), and raised the dominant intensity population from 80.10% to 97.88%. FTIR spectra revealed band displacements that align with interactions between the components. In the DPPH assay at 100–400 µg/mL, CSLNs mitigated 45.4–77.6% of radicals, while uncoated SLNs scavenged 3.6–38.4%. Chitosan treatment consequently altered the antioxidant and protein-stabilizing characteristics of the formulation in various ways, resulting in lower encapsulation estimates for CSLNs. This trade-off highlights chitosan concentration as a design variable to optimize, aiming to enhance both radical scavenging strength and oil retention. Collectively, these findings encourage the continued advancement of chitosan-treated SLNs as a potential environmentally friendly mosquito repellent; their repellent effectiveness has yet to be evaluated.

INTRODUCTION

Diseases transmitted by mosquitoes, including malaria, dengue, and filariasis, continue to be significant sources of illness, and personal protection from mosquito bites is essential for prevention. In 2024, malaria was responsible for approximately 282 million cases and 610,000 deaths globally (World Health

Organization, 2025). Synthetic repellents are effective; however, worries regarding their environmental and health impacts have prompted the exploration of natural alternatives (Wu et al., 2022). Repellents obtained from plants can rival the effectiveness of synthetic ones: a substance from lemon eucalyptus, para-menthane-3,8-diol (PMD), was evaluated against high-concentration DEET and demonstrated similar effectiveness in various assessments (Carroll & Loye, 2006). Most essential oils, however, are volatile and offer protection for brief durations, prompting the suggestion of encapsulation to delay their release and extend their protective effects (Maia & Moore, 2011). Essential oils consist of intricate combinations of volatile, lipophilic substances known for their antimicrobial, antioxidant, and anti-inflammatory properties. Their instability, tendency to oxidize, and limited solubility in water make formulation challenging. Encapsulation can enhance dispersion, safeguard delicate components, and alter the behavior of oils within a formulation.(Bakkali et al., 2008; Dupuis et al., 2022; Sousa et al., 2022).

Solid lipid nanoparticles (SLNs) are colloidal carriers at the submicron level made from lipids that stay solid at ambient and physiological temperatures, stabilized by surfactants in an aqueous medium. Their lipid matrix can interact with lipophilic substances and safeguard them (Mehnert & Mäder, 2001; Müller et al., 2000; Viegas et al., 2023). Essential oils have been incorporated into SLNs and associated lipid carriers, though payload, crystallinity, and stability differ based on composition (Carbone et al., 2018; Katopodi & Detsi, 2021). Hot homogenization in conjunction with sonication is a typical method for preparation, and variations in processing conditions significantly influence particle size and dispersity (Akbari et al., 2022; Duan et al., 2020; Khairnar et al., 2022).

Chitosan is a cationic polysaccharide, and its charge varies according to the medium's pH (Aranaz et al., 2021). Due to its biodegradability and its interactions with negatively charged interfaces, it has served as a surface modifier for nanoparticles (Aldayel et al., 2023; Burki et al., 2023; Silva et al., 2017; Wang et al., 2018; Ways et al., 2018). Chitosan-coated lipid systems have been documented for essential oil delivery and ocular transport (Aghabagherzadeh et al., 2024; Sikhondze et al., 2023), yet limited research has analyzed a multi-oil SLN prior to and following chitosan treatment through light scattering and a basic antioxidant assay.

This research had two objectives: (i) to analyze the size distribution and the UV–visible and FTIR band characteristics of both uncoated and chitosan-treated SLN dispersions with a three-oil mixture, and (ii) to evaluate their DPPH radical-scavenging capability in relation to that of ascorbic acid. The process involves a physicochemical analysis and a preliminary screening prior to any assessment of repellency.

Research question: Does chitosan treatment change the size distribution and in vitro DPPH radical-scavenging capacity of a three-oil SLN dispersion?

2. Materials and Methods

2.1 Materials and equipment

Stearic acid and glyceryl monostearate (GMS) served as solid lipids, while Tween 80 acted as the nonionic surfactant. The essential-oil phase comprised Eucalyptus globulus, Lavandula angustifolia (lavender), and Melissa officinalis (lemon balm) oils. Chitosan (low molecular weight; 50–190 kDa; degree of deacetylation ≥75%; viscosity 20–300 cP, according to the supplier), glacial acetic acid, propylene glycol, phenoxyethanol, ethanol, 2,2-diphenyl-1-picrylhydrazyl (DPPH), ascorbic acid, and distilled water were utilized. Chemicals were acquired from the University of Central Punjab's laboratory stock. An ultrasonic processor and a high-speed homogenizer were employed for emulsification and reduction of particle size. Particle size and polydispersity index were assessed using an Anton Paar Litesizer 500 (Section 2.4). FTIR spectra were obtained using an FTIR spectrophotometer, while UV–visible scans were measured with a UV–visible spectrophotometer. Standard lab apparatus consisted of a magnetic stirrer with temperature regulation, an ice bath, an analytical balance (accuracy 0.0001 g), and thermometers.

Table 1. Components of the essential-oil SLN dispersion.

Component	Role
Stearic acid	Solid lipid
Glyceryl monostearate (GMS)	Solid lipid / co-emulsifier
***Eucalyptus globulus* oil**	Essential-oil active
***Lavandula angustifolia* oil**	Essential-oil active
***Melissa officinalis* oil**	Essential-oil active
Tween 80	Surfactant
Distilled water	Aqueous phase
Phenoxyethanol	Preservative
Propylene glycol	Co-solvent / humectant
Chitosan	Surface treatment (CSLNs)
Glacial acetic acid	Chitosan solvent

2.2 Preparation of essential-oil-loaded SLNs

SLNs were created through hot-melt homogenization, a technique effective for encapsulating hydrophobic essential oils in a solid lipid matrix due to the oils easily dissolving in the melted lipid prior to emulsification (Mehnert & Mäder, 2001). The lipid phase, made up of stearic acid and GMS, was heated on a magnetic hotplate to 80 °C and maintained at this temperature for about 5 min to guarantee full melting. The essential-oil mixture (lavender, eucalyptus, and lemon balm) was subsequently added drop by drop to the melted lipid while stirring gently to ensure uniform distribution. Simultaneously, distilled water was warmed to an equivalent temperature (80 °C), and Tween 80 along with propylene glycol were mixed into it. The hot water phase was introduced gradually into the lipid phase while stirring; this slow addition aids in forming small droplets instead of large aggregates. The coarse emulsion obtained was homogenized at 30,000 rpm with 5 s on/off pulsed cycles for 2 minutes, followed by probe-sonication at 65% amplitude for 2 minutes with 5 s on/off pulses; pulsed sonication instead of continuous reduces localized heating that may harm the essential-oil components. Right after sonication, the dispersion was moved to an ice bath (0–4 °C) and stirred steadily for 15–20 min; ongoing stirring during this cooling phase aids in stopping the solidifying particles from clumping (Müller et al., 2000). After the dispersion cooled to room temperature (~25 °C), phenoxyethanol was incorporated as a preservative, the suspension was filtered using a 0.45 µm membrane to eliminate any unincorporated aggregates, and the dispersion was kept at 4 °C. The final volume was made up to 100 mL with distilled water.

2.3 Chitosan treatment

A 1% (v/v) solution of acetic acid was prepped by combining 1 mL of glacial acetic acid with 90 mL of distilled water and adjusting the total volume to 100 mL with distilled water. One gram of chitosan powder was gradually introduced to 100 mL of the solution to create a 1% (w/v) chitosan solution. The solution was mixed at 600 rpm at room temperature for 2–4 hours until it became clear. In preparing CSLN, 1 mL of the chitosan solution was gradually mixed into 5 mL of the SLN dispersion at room temperature while stirring at 550 rpm for 30 minutes. Consequently, the mixture contained around 0.17% (w/v) chitosan and 0.17% (v/v) acetic acid. CSLNs were kept at 4 °C. Uncoated control SLNs were treated with 1 mL of a 1% (v/v) acetic acid solution, excluding chitosan, under identical conditions.

2.4 Dynamic light scattering

Dynamic light scattering (Filippov et al., 2023; Jia et al., 2023) was employed to measure the hydrodynamic diameter and intensity-weighted size distributions with an Anton Paar Litesizer 500. Every sample was diluted 1:99 (v/v) using distilled water. Measurements were conducted at 25.0 °C following a 10 s equilibration period, utilizing water as the dispersant (refractive index 1.3303; viscosity 0.8903 mPa·s). Every measurement included 60 runs of 20 seconds and was analyzed using the cumulant model.

2.5 FTIR spectroscopy

FTIR spectra were obtained for the essential-oil mixture, chitosan, uncoated SLNs, and CSLNs as liquid (aqueous) samples, across a range of about 4000–600 cm^{-1}. Because water absorption coincides with the O–H/N–H and amide I regions, band positions were assessed qualitatively only.

2.6 UV–visible profile

A UV–visible scan of the uncoated SLN dispersion was performed in the range of about 200 to 450 nm, with absorbance values measured at 210, 265, and 290 nm. The scan is described in detail and was not utilized for measuring oil content.

2.7 DPPH radical-scavenging assay

DPPH radical scavenging was assessed using DPPH (0.1 mM; 3.9 mg in 100 mL ethanol) and ascorbic acid as the positive control (Brand-Williams et al., 1995). Dispersions of uncoated SLN and CSLN were evaluated at concentrations of 100, 200, 300, and 400 µg/mL, with absorbance measured at 517 nm following a 30-minute incubation in the dark at room temperature. The expression of inhibition is based on the work of Gulcin and Alwasel (2023) as well as Kedare and Singh (2011):

DPPH scavenging (%) = (A_DPPH − A_sample) / A_DPPH × 100 (Gulcin & Alwasel, 2023; Kedare & Singh, 2011)

where A_DPPH is the absorbance of DPPH without sample (0.4487) and A_sample is the absorbance of the tested sampleAll samples and the ascorbic acid control were assessed in one session on the same day, using the same DPPH standard. Each concentration was assessed three times.

2.8 Data reporting

Values are presented as mean ± SD based on triplicate DPPH measurements from a single preparation batch. These replicates assess analytical repeatability rather than variability between batches; hence, no inferential tests are presented and no conclusions at the batch level are made.

3. Results

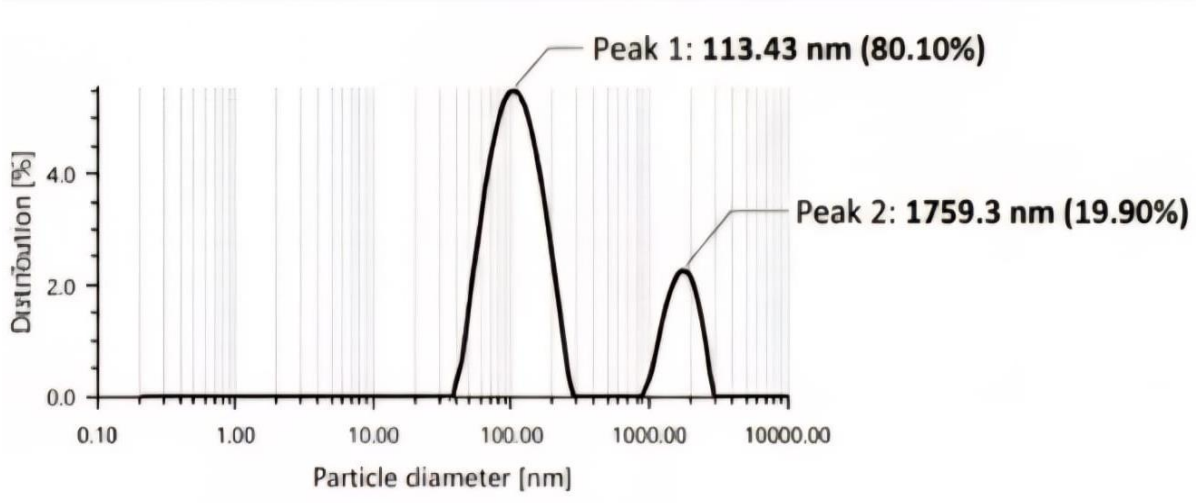
3.1 Particle-size distribution

Uncoated SLNs exhibited a Z-average hydrodynamic diameter of 410.3 nm along with a PDI of 0.216. The intensity distribution revealed a primary peak at 113.4 nm (80.1% of intensity) and a secondary peak at 1759 nm (19.9%). CSLNs exhibited a Z-average of 245.2 nm and a PDI of 0.163, showing a prominent peak at 176.0 nm (97.9%) and a smaller peak at 2435 nm (2.1%) (Table 2; Figure 1). Every value corresponds to an individual measurement from one batch of each formulation, and the two formulations were assessed under varying cell and scattering conditions (Section 2.4). The primary peak moved from 113 to 176 nm, thus the decreased Z-average primarily indicates a smaller proportion of the large-particle

population (19.9% versus 2.1% by intensity), rather than a consistent decrease in particle size. Intensity weighting exaggerates the representation of large particles, and distributions based on number were not achieved.

Table 2. DLS results for uncoated SLNs and CSLNs. Single measurement from one batch for each formulation.

Parameter	Uncoated SLNs	CSLNs
Z-average hydrodynamic diameter	410.3 nm	245.2 nm
Polydispersity index (PDI, dimensionless)	0.216	0.163
Dominant intensity peak	113.43 nm	176.01 nm
Dominant peak area	80.10%	97.88%
Secondary peak	1759.3 nm	2435 nm
Secondary peak area	19.90%	2.12%
Peak width (instrument SD), peak 1	44.84 nm	75.84 nm
Peak width (instrument SD), peak 2	444.2 nm	584.6 nm



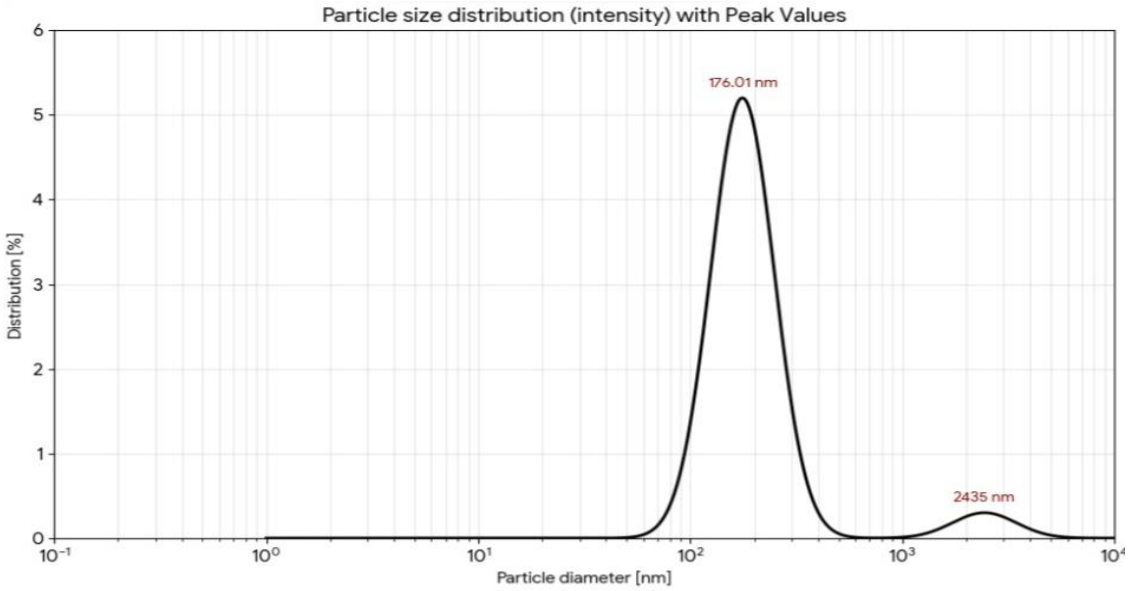


Figure 1. Intensity-weighted particle-size distributions of uncoated SLNs (a) and CSLNs (b), measured by DLS at 25 °C. Dominant peaks are 113.43 nm (80.10%) and 1759.3 nm (19.90%) for uncoated SLNs, and 176.01 nm (97.88%) and 2435 nm (2.12%) for CSLNs.

3.2 FTIR spectra

Positions of the bands varied somewhat among the essential-oil mixture, chitosan, uncoated SLNs, and CSLNs (Table 3; Figure 2). The wide O–H/N–H band shifted approximately 12 cm^{-1} (from 3308 to 3296 cm^{-1}) and the amide I band shifted by around 2 cm^{-1} (from 1638 to 1636 cm^{-1}) between uncoated SLNs and CSLNs. The spectrum of the uncoated SLN showed a baseline shift and lacked distinct fingerprint bands, restricting comparisons to the broader and amide areas. Shifts of this magnitude are minimal, therefore FTIR is presented descriptively and is not construed as proof of molecular interaction.

Table 3. Selected FTIR minima.

Sample	Broad region	1600–1700 cm^{-1} region	Selected fingerprint features
Essential-oil blend	3386	1673	1245, 1090, 1047
Chitosan	3277	1638	—
Uncoated SLNs	3308	1638	—
CSLNs	3296	1635	1074

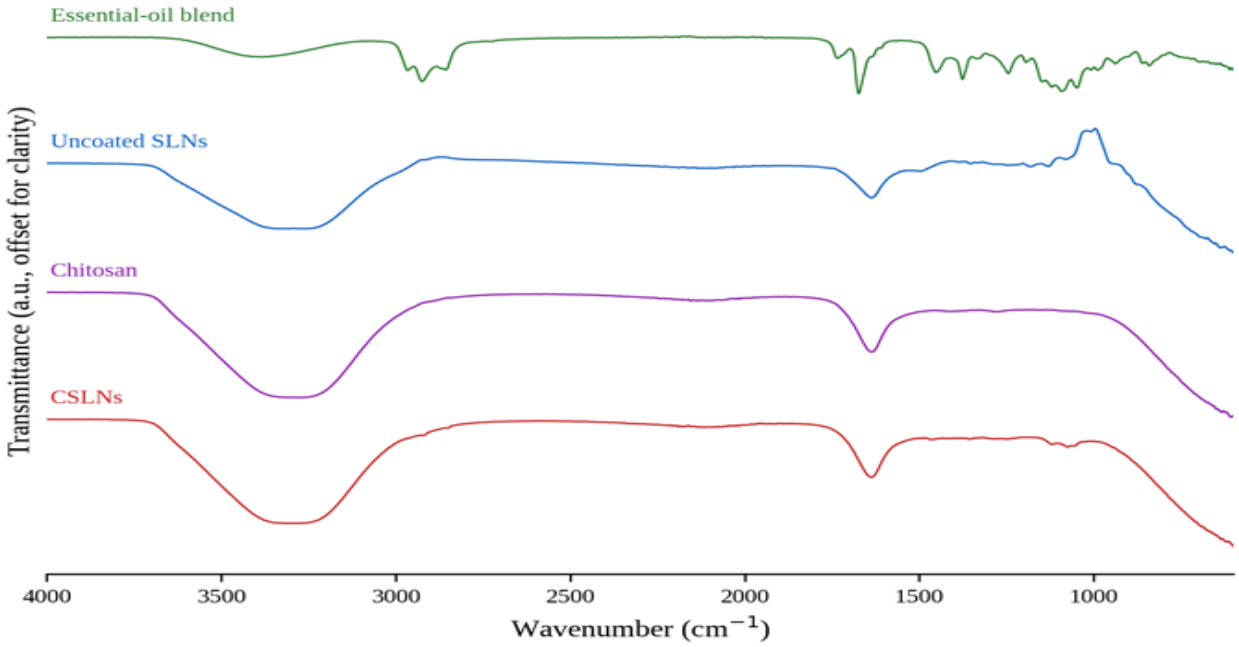
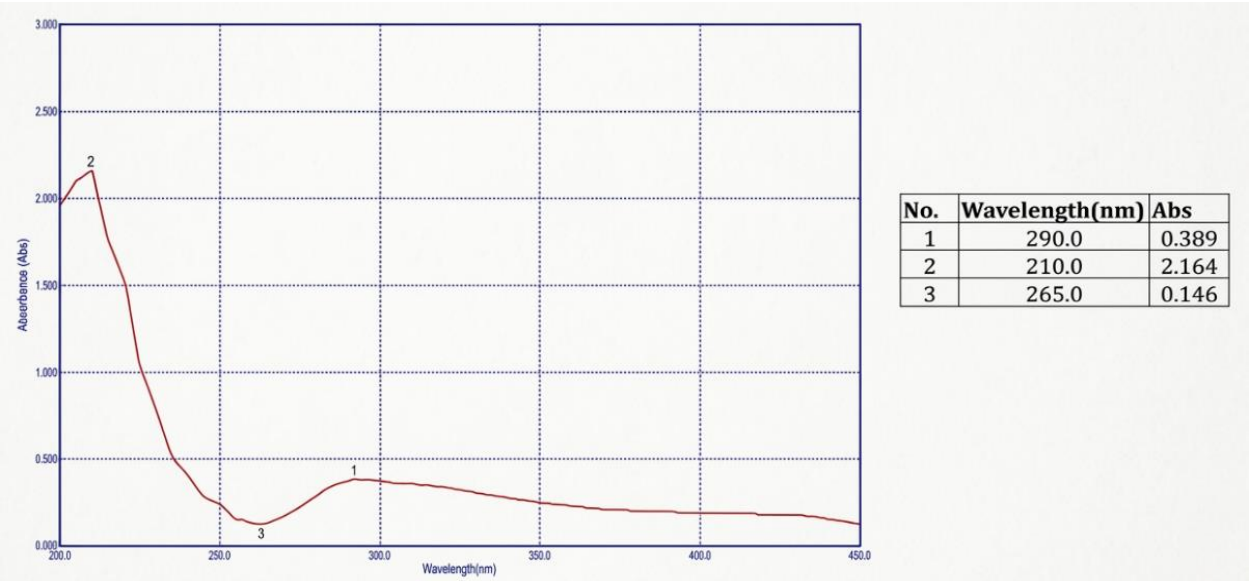


Figure 2. FTIR spectra of the essential-oil blend, chitosan, uncoated SLNs, and CSLNs, shown with vertical offsets for clarity.

3.3 UV–visible profile

The UV–visible spectrum of the uncoated SLN dispersion exhibited absorbance values of 2.164 at 210 nm, 0.146 at 265 nm, and 0.389 at 290 nm (Figure 3). The profile is described in detail. Due to the weak chromophores in this region of the essential oils and the presence of other absorbing components in the dispersion, these values were not utilized to assess oil content or encapsulation.



No.	Wavelength(nm)	Abs
1	290.0	0.389
2	210.0	2.164
3	265.0	0.146

Figure 3. UV–visible wavelength scan (200–450 nm) of the uncoated SLN dispersion, with readings at 210 nm (A = 2.164), 265 nm (A = 0.146), and 290 nm (A = 0.389).

Table 4. DPPH radical scavenging at 517 nm across 100–400 µg/mL. Absorbance and scavenging values are shown as mean ± SD.

Concentration (µg/mL)	CSLN absorbance (mean ± SD)	CSLN scavenging (%)	Uncoated SLN absorbance (mean ± SD)	Uncoated SLN scavenging (%)	Ascorbic acid absorbance (mean ± SD)	Ascorbic acid scavenging (%)
100	0.2450 ± 0.0008	45.4 ± 0.2	0.3330 ± 0.0001	25.8 ± 0.0	0.0414 ± 0.0003	90.8 ± 0.1
200	0.1594 ± 0.0002	64.5 ± 0.0	0.4323 ± 0.0089	3.6 ± 2.0	0.0401 ± 0.0002	91.1 ± 0.0
300	0.1005 ± 0.0000	77.6 ± 0.0	0.2762 ± 0.0018	38.4 ± 0.4	0.0223 ± 0.0007	95.0 ± 0.2
400	0.1004 ± 0.0002	77.6 ± 0.0	0.3046 ± 0.0037	32.1 ± 0.8	0.0257 ± 0.0006	94.3 ± 0.1

3.4 DPPH radical scavenging

CSLNs scavenged more DPPH radicals than uncoated SLNs at all tested concentrations (100–400 µg/mL), achieving a plateau of 77.6% at 300 and 400 µg/mL, suggesting that the scavenging ability was nearly saturated at these levels (Table 4; Figure 4). Uncoated SLNs scavenged between 3.6% and 38.4%, reaching a maximum of 300 µg/mL, and the response varied non-monotonically with concentration; this has been documented. Ascorbic acid, serving as the positive control, yielded 90.8–95.0%. All values were determined relative to the same DPPH-only reference absorbance (0.4487), and both formulations were assessed in a single run on the same day, in triplicate.

Scavenging was calculated against a DPPH-only reference absorbance of 0.4487. All samples and the ascorbic acid control were measured in a single run.

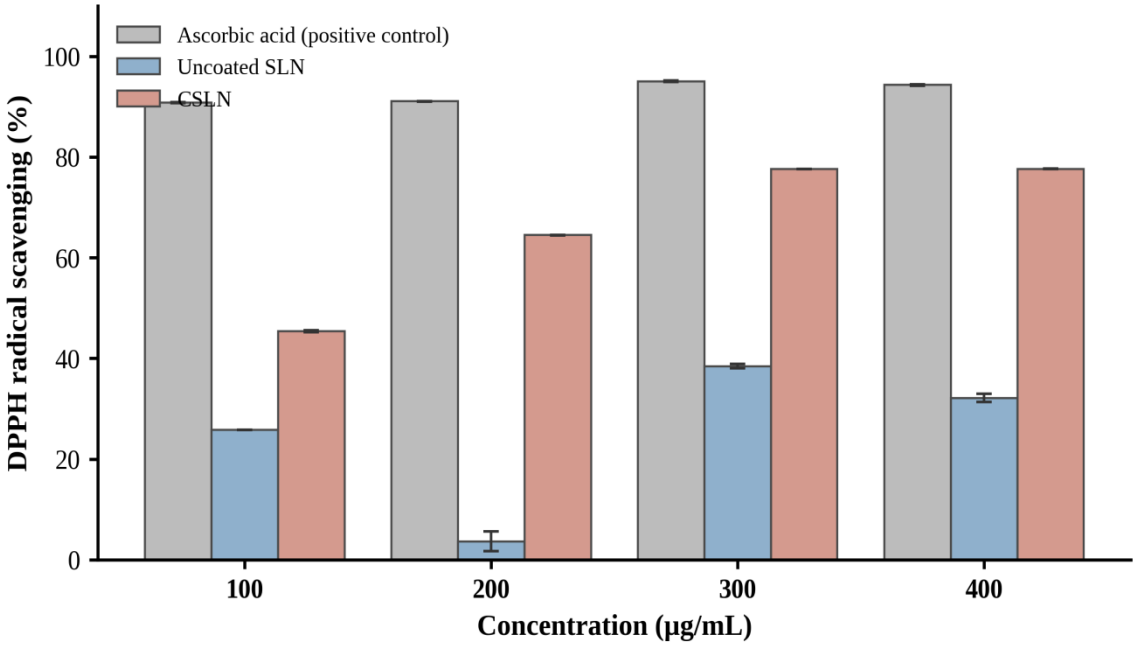


Figure 4. DPPH radical scavenging of uncoated SLNs, CSLNs, and ascorbic acid (positive control) at 100–400 µg/mL, measured at 517 nm. Error bars show the standard deviation of replicate sample absorbance, propagated to percent scavenging.

4. Discussion

The DLS data align with a shift in the size distribution following chitosan treatment, each formulation was assessed once from a single batch. The movement of the primary peak from 113 to 176 nm, along with the alteration in the mass of the large-particle group, would gain from validation through number-weighted analysis and electron microscopy in subsequent studies.

CSLNs exhibited greater DPPH scavenging compared to uncoated SLNs across all tested concentrations. This study did not include a control with only chitosan; incorporating one in future research would clarify if the polymer alone affects the signal. Constituents of essential oils are also noted to be reactive to radicals (Bakkali et al., 2008), and they might play a role in the signal for both formulations. The observed non-monotonic response of uncoated SLNs is documented here, and understanding its cause will necessitate testing over several batches and days.

The reasoning behind the repellent is a theory. The PMD research (Carroll & Loye, 2006) pertains to a compound from Corymbia citriodora (lemon eucalyptus), not E. globulus; thus it advocates for plant-based repellents by analogy instead of providing direct evidence for the oil blend utilized here. Wu et al. (2022) documented the repellent properties of essential oils and their components against Aedes albopictus. The current formulation has not been evaluated for repellency, and no claims of repellency are made. A WHO-compliant test would be necessary prior to any comparison with synthetic repellents. This study presents an initial physicochemical and antioxidant analysis of a single batch from each formulation, laying the groundwork for future research on encapsulation, repellent effectiveness, and antioxidant properties in biological contexts.

5. Limitations

- This research is initial and restricted to a single batch for each formulation, with DLS and DPPH each evaluated once per condition. The two DLS measurements were conducted under varying cell and scattering conditions. Zeta potential, validated oil loading (GC or GC–MS), and microscopy were not conducted, thus the chitosan layer and encapsulation remain unverified. FTIR was obtained from aqueous samples and is utilized solely for qualitative analysis. The testing of repellent activity, oil release, and storage stability was not conducted.

6. Conclusion

In each formulation batch, chitosan treatment resulted in a reduced Z-average diameter and a decreased PDI, along with enhanced in vitro DPPH radical scavenging. These results are initial. Future studies need to incorporate independent batches, zeta potential assessments, and electron microscopy, confirmed quantification of oil loading via GC or GC–MS, a chitosan-only DPPH control, investigations on storage stability and release, as well as repellency tests prior to asserting any claims regarding repellent activity.

Declarations

Funding: No specific funding was received for this work. **Conflict of interest:** The authors declare no conflicts of interest. **Data availability:** Raw replicate data are available from the corresponding author on request.

REFERENCES

Aghabagherzadeh, M., Karimi, E., & Zareian, M. (2024). Folic acid-conjugated chitosan-coated solid lipid nanoparticles: Precision targeting of *Artemisia vulgaris* essential oils for anticancer therapy. *Chemistry & Biodiversity, 21*(1), Article e202300187. https://doi.org/10.1002/cbdv.202300187

Akbari, J., Saeedi, M., Ahmadi, F., Hashemi, S. M. H., Babaei, A., Yaddollahi, S., Rostamkalaei, S. S., Asare-Addo, K., & Nokhodchi, A. (2022). Solid lipid nanoparticles and nanostructured lipid carriers: A review of the methods of manufacture and routes of administration. *Pharmaceutical Development and Technology, 27*(5), 525–544. https://doi.org/10.1080/10837450.2022.2084554

Aldayel, T. S., Badran, M. M., Alomrani, A. H., AlFaris, N. A., Altamimi, J. Z., Alqahtani, A. S., Nasr, F.

A., Ghaffar, S., & Orfali, R. (2023). Chitosan-coated solid lipid nanoparticles as an efficient avenue for boosted biological activities of *Aloe perryi*: Antioxidant, antibacterial, and anticancer potential. *Molecules, 28*(8), Article 3569. https://doi.org/10.3390/molecules28083569

Aranaz, I., Alcántara, A. R., Civera, M. C., Arias, C., Elorza, B., Heras Caballero, A., & Acosta, N. (2021). Chitosan: An overview of its properties and applications. *Polymers, 13*(19), Article 3256. https://doi.org/10.3390/polym13193256

Bakkali, F., Averbeck, S., Averbeck, D., & Idaomar, M. (2008). Biological effects of essential oils—A review. *Food and Chemical Toxicology, 46*(2), 446–475. https://doi.org/10.1016/j.fct.2007.09.106

Brand-Williams, W., Cuvelier, M. E., & Berset, C. (1995). Use of a free radical method to evaluate antioxidant activity. *LWT - Food Science and Technology, 28*(1), 25–30. https://doi.org/10.1016/S0023-6438(95)80008-5

Burki, F. A., Shah, K. U., Razaque, G., Shah, S. U., Nawaz, A., Saeed, M. D., Rehman, M. U., Bibi, H., Alfatama, M., & Elsayed, T. M. (2023). Optimization of chitosan-decorated solid lipid nanoparticles for improved flurbiprofen transdermal delivery. *ACS Omega, 8*(22), 19302–19310. https://doi.org/10.1021/acsomega.2c08135

Carbone, C., Martins-Gomes, C., Caddeo, C., Silva, A. M., Musumeci, T., Pignatello, R., Puglisi, G., & Souto, E. B. (2018). Mediterranean essential oils as precious matrix components and active ingredients of lipid nanoparticles. *International Journal of Pharmaceutics, 548*(1), 217–226. https://doi.org/10.1016/j.ijpharm.2018.06.064

Carroll, S. P., & Loye, J. (2006). PMD, a registered botanical mosquito repellent with deet-like efficacy. *Journal of the American Mosquito Control Association, 22*(3), 507–514. https://doi.org/10.2987/8756-971X(2006)22[507:PARBMR]2.0.CO;2

Duan, Y., Dhar, A., Patel, C., Khimani, M., Neogi, S., Sharma, P., Siva Kumar, N., & Vekariya, R. L. (2020). A brief review on solid lipid nanoparticles: Part and parcel of contemporary drug delivery systems. *RSC Advances, 10*(45), 26777–26791. https://doi.org/10.1039/d0ra03491f

Dupuis, V., Cerbu, C., Witkowski, L., Potarniche, A. V., Timar, M. C., Żychska, M., & Sabliov, C. M. (2022). Nanodelivery of essential oils as efficient tools against antimicrobial resistance: A review of the type and physical-chemical properties of the delivery systems and applications. *Drug Delivery, 29*(1), 1007–1024. https://doi.org/10.1080/10717544.2022.2056663

Filippov, S. K., Khusnutdinov, R., Murmiliuk, A., Inam, W., Zakharova, L. Y., Zhang, H., & Khutoryanskiy, V. V. (2023). Dynamic light scattering and transmission electron microscopy in drug delivery: A roadmap for correct characterization of nanoparticles and interpretation of results. *Materials Horizons, 10*(12), 5354–5370. https://doi.org/10.1039/d3mh00717k

Gulcin, İ., & Alwasel, S. H. (2023). DPPH radical scavenging assay. *Processes, 11*(8), Article 2248. https://doi.org/10.3390/pr11082248

Jia, Z., Li, J., Gao, L., Yang, D., & Kanaev, A. (2023). Dynamic light scattering: A powerful tool for in situ nanoparticle sizing. *Colloids and Interfaces, 7*(1), Article 15. https://doi.org/10.3390/colloids7010015

Katopodi, A., & Detsi, A. (2021). Solid lipid nanoparticles and nanostructured lipid carriers of natural products as promising systems for their bioactivity enhancement: The case of essential oils and flavonoids. *Colloids and Surfaces A: Physicochemical and Engineering Aspects, 630*, Article 127529. https://doi.org/10.1016/j.colsurfa.2021.127529

Kedare, S. B., & Singh, R. P. (2011). Genesis and development of DPPH method of antioxidant assay. *Journal of Food Science and Technology, 48*(4), 412–422. https://doi.org/10.1007/s13197-011-0251-1

Khairnar, S. V., Pagare, P., Thakre, A., Nambiar, A. R., Junnuthula, V., Abraham, M. C., Kolimi, P., Nyavanandi, D., & Dyawanapelly, S. (2022). Review on the scale-up methods for the preparation of solid lipid nanoparticles. *Pharmaceutics, 14*(9), Article 1886. https://doi.org/10.3390/pharmaceutics14091886

Maia, M. F., & Moore, S. J. (2011). Plant-based insect repellents: A review of their efficacy, development and testing. *Malaria Journal, 10*(Suppl 1), Article S11. https://doi.org/10.1186/1475-2875-10-S1-S11

Mehnert, W., & Mäder, K. (2001). Solid lipid nanoparticles: Production, characterization and applications. *Advanced Drug Delivery Reviews, 47*(2–3), 165–196. https://doi.org/10.1016/s0169-409x(01)00105-3

Müller, R. H., Mäder, K., & Gohla, S. (2000). Solid lipid nanoparticles (SLN) for controlled drug delivery—A review of the state of the art. *European Journal of Pharmaceutics and Biopharmaceutics, 50*(1), 161–177. https://doi.org/10.1016/s0939-6411(00)00087-4

Sikhondze, S. S., Makoni, P. A., Walker, R. B., & Khamanga, S. M. M. (2023). Chitosan-coated SLN: A potential system for ocular delivery of metronidazole. *Pharmaceutics, 15*(7), Article 1855. https://doi.org/10.3390/pharmaceutics15071855

Silva, M. M., Calado, R., Marto, J., Bettencourt, A., Almeida, A. J., & Gonçalves, L. M. D. (2017). Chitosan nanoparticles as a mucoadhesive drug delivery system for ocular administration. *Marine Drugs, 15*(12), Article 370. https://doi.org/10.3390/md15120370

Sousa, V. I., Parente, J. F., Marques, J. F., Forte, M. A., & Tavares, C. J. (2022). Microencapsulation of essential oils: A review. *Polymers, 14*(9), Article 1730. https://doi.org/10.3390/polym14091730

Viegas, C., Patrício, A. B., Prata, J. M., Nadhman, A., Chintamaneni, P. K., & Fonte, P. (2023). Solid lipid nanoparticles vs. nanostructured lipid carriers: A comparative review. *Pharmaceutics, 15*(6), Article 1593. https://doi.org/10.3390/pharmaceutics15061593

Wang, F.-z., Zhang, M.-w., Zhang, D.-s., Huang, Y., Chen, L., Jiang, S.-m., Shi, K., & Li, R. (2018). Preparation, optimization, and characterization of chitosan-coated solid lipid nanoparticles for ocular drug delivery. *Journal of Biomedical Research, 32*(6), 411–423. https://doi.org/10.7555/jbr.32.20160170

Ways, T. M. M., Lau, W. M., & Khutoryanskiy, V. V. (2018). Chitosan and its derivatives for application in mucoadhesive drug delivery systems. *Polymers, 10*(3), Article 267. https://doi.org/10.3390/polym10030267

World Health Organization. (2025). *World malaria report 2025: Partner briefing*. https://cdn.who.int/media/docs/default-source/malaria/world-malaria-reports/world-malaria-report-2025-partner-briefing-eng.pdf

Wu, W., Yang, Y., Feng, Y., Ren, X., Li, Y., Li, W., Huang, J., Kong, L., Chen, X., Lin, Z., Hou, X., Zhang, L., Chen, Y., Sheng, Z., & Hong, W. (2022). Study of the repellent activity of 60 essential oils and their main constituents against *Aedes albopictus*, and nano-formulation development. *Insects, 13*(12), Article 1077. https://doi.org/10.3390/insects13121077